Nationaal Lucht- en Ruimtevaartlaboratorium
National Aerospace Laboratory NLR

NLR-TP-98629

Modelling the effects of operating conditions and alternative fuels on gas turbine performance and emissions

W.P.J. Visser and S.C.A. Kluiters

Nationaal Lucht- en Ruimtevaartlaboratorium
National Aerospace Laboratory NLR

NLR-TP-98629

Modelling the effects of operating conditions and alternative fuels on gas turbine performance and emissions

W.P.J. Visser and S.C.A. Kluiters

This report is based on a presentation held at the RTO-AVT "Gas Turbine Engine Combustion, Emissions and Alternative Fuels" symposium, Lisbon, Portugal, 12-16 October 1998.

Division:	Flight
Issued:	December 1998
Classification of title:	unclassified

Summary

With the increasing attention to gas turbine exhaust gas pollution, a need has emerged to assess effects of a variety of operational variables on the emission levels. An effective approach to address this need is to integrate combustor emission models in gas turbine performance models.
NLR's generic gas turbine performance simulation environment (GSP) has therefore been extended with a number of features for accurate analysis of these effects on the major exhaust gas emissions NO_x, CO, UHC and Smoke. First, GSP's gas model has been extended to include a detailed description of gas composition including the particular emission species. Second, a new generic multi-reactor combustor model has been developed for detailed modelling of the processes in a combustor. The combustor model is set up by defining a number of reactors modelling combustion, mixing, steam/water-injection and their effects on emission formation using semi-empirical models for the reaction kinetics. Fuel properties and composition can be specified in detail, enabling analysis of effects of alternative fuels on gas turbine engine performance and emissions.
Preliminary validation results with the multi-reactor combustion model corresponded with measured emission data and with expected operating condition effects on emissions. With the NO_x model best accuracy was obtained. The accuracy of particularly the CO, UHC and Smoke formation models may be improved by adapting the multi-reactor model to allow for modelling of effects such as film cooling and other effects not covered by a one-dimensional model.
The current generic multi-reactor combustor module will be used for easy implementation of improved emission models in the future. This work will also involve extensive validation using detailed engine, combustor and emission data.

This page was intentionally left blank

Contents

(33 pages in total)

Nomenclature

ϕ	equivalence ratio	
EI	Emission Index	
ETA	efficiency	
GSP	NLR Gas turbine Simulation Program	
LCV	Low Calorific Value fuel	
LH_2	liquefied hydrogen	
LNG	liquefied natural gas	
LPP	Lean Premixed Pre-evaporated combustion	
Ma	Mach number	
p	pressure	
Pnetc	Net (fuel compression corrected) power output	
ppm	parts per million	
RQL	Rich Quick-quench Lean combustion	
S	Soot formation concentration	[mg/kg gas]
SN	Smoke number	
T	Temperature	[K]
UHC	Unburnt HydroCarbons	
X	mole fraction	
[X]	mole (volume) concentration	[kmole/m^3]
W	mass flow rate	[kg/s]
Wf	Fuel mass flow rate	[kg/s]
ω	Specific surface oxidation rate	[g/cm^2/s]

indices

CH	hydrocarbon
eq	(chemical) equilibrium
f	fuel
ox	oxidant
pz	primary zone
stoïch	stoïchiometric (fuel-air ratio)

1 Introduction

With the increasing attention to gas turbine exhaust gas pollution, a need has emerged to predict gas turbine exhaust gas emission levels at varying operating conditions. On the manufacturers side, the processes in the combustor are modeled in detail (i.e. with CFD) in order to develop new technologies to reduce emissions, such as LPP and RQL combustion (e.g. Schumann [33]). On the operational side, there is interest in how to minimize emissions by optimizing operating conditions such as engine condition, aircraft flight procedures, fuel type and water/steam injection. The latter two variables mainly relate to ground based gas turbines, using LNG, LH_2 or fuel obtained from gasification of coal or bio-mass. However, it must be noted that LNG and LH_2 fuels for aircraft are already being considered (Pohl [28]).

NLR contributes to several programs directed at more accurate assessment of gas turbine exhaust gas emissions and their effects on the environment, using test-bed and in-flight measurements (Jentink [16]) and prediction with models. For developing accurate models to predict emissions at deviating operating conditions, accurate measurement methods are required for validation.

An effective approach to analyze operating conditions effects on emissions is to integrate emission models in gas turbine performance models like NLR's Gas turbine Simulation Program GSP [37]. A lot of work has already been performed modelling the processes in the combustor in order to predict emissions, ranging from simple relations between engine performance parameters and emission levels (0-dim parametric models, Kretschmer [19] and Rizk [30]) to complex CFD computations (e.g. Maidhof [23]). Especially the more simple, often empirical, models require some sort of calibration to a reference condition before they can be used for sensitivity analysis, so they can be referred to as "off-design" or "ratio" models (Schumann [34]). For accurate direct prediction of emissions without any reference data, CFD calculations will be required. It must be noted that best results with combustion CFD modeling still are "suffering" from inaccuracies in the order of 10-30%.

Ratio models can easily be implemented in an engine performance model in order to provide a tool to directly relate operating condition (via combustor operating condition) to emission level. However, the potential of the single equation ratio models to analyze a large variety of effects is very limited.

In order to obtain better insight in effects of using other fuels, deviating air properties, water injection etc. a more detailed model is required. Yet, integration of CFD computations in GSP was not considered feasible due to the disproportional complexity and computing power requirement of CFD in relation to the 0-dimensional GSP model.

A compromise between the CFD models and the simple empirical models are multi-reactor models, which apply a limited degree of spatial differentiation inside the combustor. Multi-reactor models usually include separate flow and chemical models and offer a means to

calculate a number of intermediate temperatures along the combustion process such as primary and dilution zone temperatures.

The simplest *combustor flow models* employ “well-stirred” reactors, assuming immediate mixing of separate user defined reactant flows. Explicit modelling of the distribution of cooling flows and the mixing processes involves a significant increase in complexity (e.g. multi-dimensional models).

Simple *chemical models* assume complete combustion in each reactor (no dissociation). Higher fidelity is obtained when calculating chemical equilibrium and best 1-dimensional detail is obtained when calculating chemical kinetics (Rodriguez [31]; Bozza [5]).

A considerable number of publications suggest the value of multi-reactor models for prediction of especially NO_x emissions (Botros [4]; Bozza [5]). These models include detailed fuel and gas composition data and NO_x formation kinetics.

This approach was considered as the best trade-off between model fidelity, complexity and computing power requirements, and has been employed in the work described below. An important presumption was that the model would primarily be used to calculate deviations of emissions from predefined reference values at reference engine conditions.

2 NLR Gas turbine Simulation Program GSP

NLR's primary tool for gas turbine engine performance analysis is the "Gas turbine Simulation Program" (GSP) [37]. Both steady-state and transient simulation of any kind of gas turbine configuration can be performed by establishing a specific arrangement of engine component modules. GSP is a powerful tool for analysis of effects of ambient and flight conditions, installation losses, deterioration and malfunctions of control- and other subsystems on performance.

During continuous development at NLR, GSP has been extended and improved with new features for specific applications. A significant improvement has been the conversion (from mainframe) to the Windows95/NT platform, enabling execution on PC's which currently offer sufficient power to perform the extensive thermodynamic calculations.[1]

GSP is now implemented in the Borland Delphi object oriented development environment, offering excellent means to maintain and extend the program.

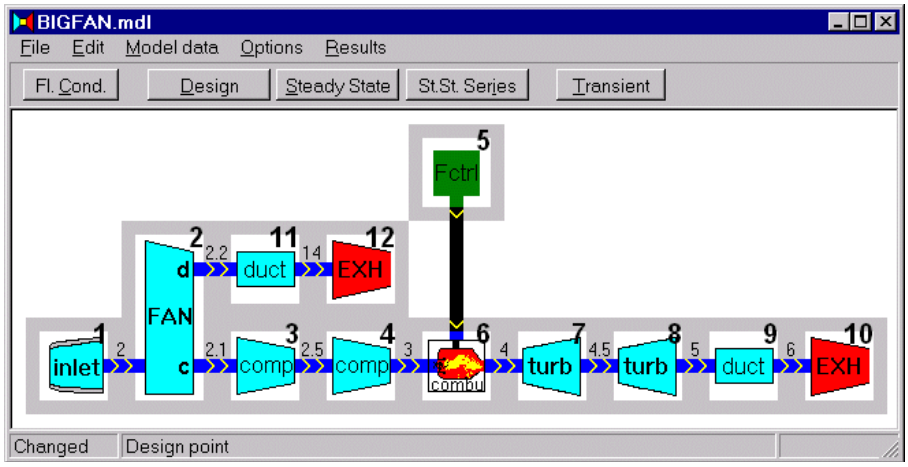

Figure 1 GSP model window with simple turbofan model

With Windows95/NT, GSP has a user friendly drag&drop graphical user interface, allowing quick implementation of new engine models and quick analysis of complex problems. In section 7, examples of GSP output are shown.

The current object oriented structure offers excellent opportunity to implement new developed models of subsystems, such as combustor/emission models. Where necessary for particular analysis problems, new or modified component models can easily be derived from existing ones using inheritance.

[1] A demo copy of GSP can be downloaded from http://www.nlr.nl/public/facilities/f141-01/index.html

3 Gas model

A first improvement necessary to be able to calculate the combustion process in more detail is a gas model including detailed accounting of gas composition, and the implementation of the equations for chemical equilibrium to calculate dissociation effects and effects of evaporation of injected water. This, combined with a detailed specification of fuel composition provides a means to calculate effects of fuel and gas composition and water or steam injection on gas turbine performance.

The resulting "global" gas model is now used throughout the entire engine cycle calculation and currently includes the following species: CO_2, CO, O_2, Ar, H_2O(gas), H_2O(liquid), H_2, CH_4, C_2H_6, C_2H_4, C_3H_8, C_4H_{10}, O, H, OH, NO, N_2O, N_2.

Chemical equilibrium is calculated for the CO_2-CO-O_2-H_2O-H_2 system:

$$CO_2 \leftrightarrow CO + \frac{1}{2}O_2 \qquad (1)$$

$$H_2O \leftrightarrow H_2 + \frac{1}{2}O_2 \qquad (2)$$

For water, also the vapor-liquid equilibrium is calculated.

In the combustor, a more detailed gas model is used, calculating equilibrium for CO_2, CO, O_2, O, H_2O, H_2, H, OH, NO, N_2O, N_2.

An efficient algorithm was developed to calculate the equilibrium using the equilibrium constants method (Kuo [20], Glassman [10]) thereby avoiding explicit solution of the Gibb's equations like in the NASA CEA program (Gordon, McBride [11, 24]).

4 Fuel specification

In order to maintain proper bookkeeping of the composition downstream of the combustor, also specification of fuel composition is required. Therefore GSP was extended with a flexible user interface module for fuel properties with either:

- specification of hydrogen/carbon (H/C) ratio and heating value, or,
- explicit specification of composition.

For fuels with many different species like jet fuels, specification of all specie concentrations is unpractical and the H/C ratio option is used with the heating value specified. This option also allows for easy specification of other fuels whose composition is unknown or complex. The resulting combustion gas composition is calculated using the H/C ratio.

For fuels with a limited number of species, the composition can be specified explicitly (per specie) and the heat release can directly be calculated from the heat of reaction (changes in formation enthalpies) and the enthalpies of the reactants, using the NASA CEA program data [11, 24]. This option enables the user to specify exotic fuels such as those generated with bio-mass gasification and allows for detailed analysis of effects of alternative fuels on performance and emissions, taking the effects of deviations in combustion gas properties fully into account.

Other fuel properties to be specified include pressure and temperature and data to calculate fuel pump compression power.

5 Combustor model

For gas turbine performance analysis, the combustor model must accurately calculate both heat release and combustor exit gas composition. Heat release is calculated assuming the combustion ends with chemical equilibrium, as calculated with the gas model described in section 3.
If the chemical equilibrium equations include terms for NO_x, CO, and UHC emission species, then the equilibrium emission values in a combustion process can be calculated. However, due to the rapid variation of gas conditions (temperatures etc.) in the combustion process, the formation of these emissions is highly subject to chemical kinetics, resulting in emissions significantly deviating from equilibrium, like "frozen" NO_x after rapid cooling of hot gas. Thus, the model should include kinetics to calculate the emission reaction rates.
In order to account for different reaction rates in the different combustor zones, the multi-reactor approach is required.

5.1 Generic multi-reactor model

A generic reactor model was developed, allowing the calculation of both chemical equilibrium and kinetics between reactor entry and exit (see fig. 2). The reactor receives the gas from a preceding reactor and exits into a successive reactor (the first and the last reactors will usually connect to compressor discharge and turbine entry instead, like in figure 3). A second reactor entry permits the injection of fuel, cooling air, gas, water or other matter to be mixed or combusted in the reactor.
By stacking a number of reactors, a multi-reactor model is obtained simulating the subsequent processes of flow-dividing, combustion, secondary combustion, mixing and, if desired, the injection of other species such as water or steam.

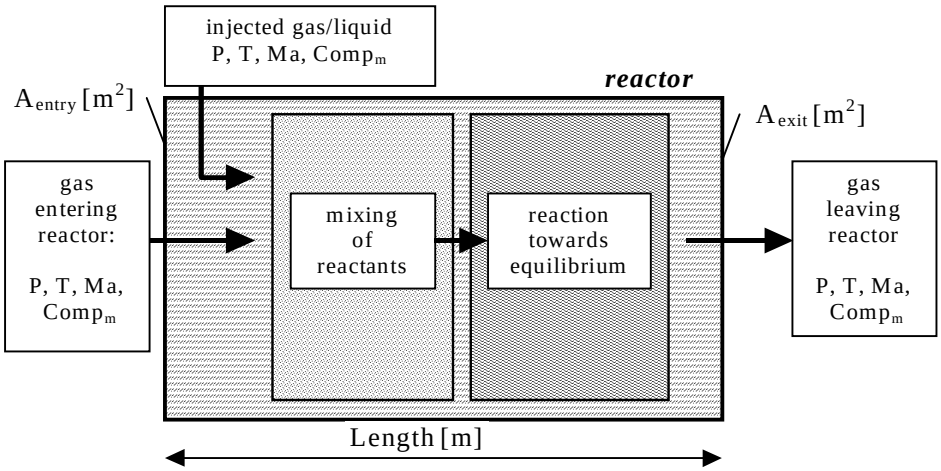

Figure 2 Generic 1-dim reactor model

Any number of reactors, each with specific characteristics, can be specified. For a conventional combustor the first reactor would represent the primary combustion zone followed by one or two reactors for the secondary or tertiary (mixing) zones (see the two-reactor model in figure 3). For detailed analysis of emissions or for multi-stage combustors, more reactors can be added.

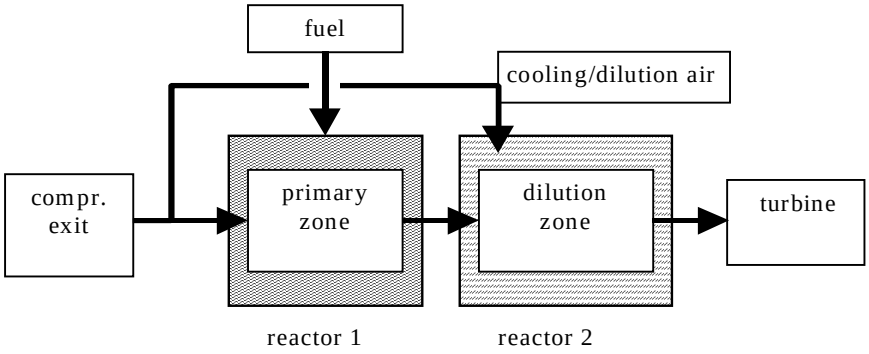

Figure 3 Simple multi-reactor configuration for a conventional combustor

5.2 Flow model

The flow model represents the distribution of the flows over the different reactors defined for the combustor. Mixing is assumed to occur instantaneously (i.e. well stirred reactors). The detailed combustor data necessary to determine flow distribution often are hard to obtain. For a fixed operating point of a conventional combustor model, a reasonable estimate can be made of the portion of total compressor air flow entering the primary combustion zone (i.e. the first reactor), which determines the primary zone equivalence ratio. However, to predict how this ratio will change with changes in power setting or other operating conditions, is difficult unless CFD flow models are used. It is therefore decided to use fixed user defined ratios for the moment. Future research will be directed at an attempt to find relatively simple 1-dim models for this effect using parametric models of the aerodynamics of the cooling flows (e.g. using equations suggested by Lefebvre [22]).

The limitation of user defined fixed flow ratios implies that validity of the model may well degrade with large deviations from the reference operating point (especially deviating total airflow rate).

5.3 Chemical model

The chemical model calculates chemical equilibrium (for heat release) and a kinetic scheme for emissions.

5.3.1 Heat release calculation

The combustion heat release is calculated assuming instantaneous attainment of chemical equilibrium. This can be justified by the fact that hydrocarbon reactions generally are rapid (see for example Sturgess [35]). Justification for this assumption can also be found in Hammond [12], who compared application of kinetic schemes with an equilibrium model. Conclusions were that for the exact determination of the composition, an equilibrium model could not be used, but the completeness of combustion and the temperature (i.e. heat release) could be fairly well approximated with the equilibrium assumption.

5.3.2 Emission calculations

The formation of all four emissions of interest (NO_x, CO, UHC and Smoke) is modeled using the same generic approach, assuming two separate mechanisms. The first mechanism is "prompt" emission formation in a flame in an infinitely short time. The second mechanism is the subsequent change in emission concentrations due to chemical reactions during the flow through the successive reactors. This way of modelling reaction kinetics (the kinetic scheme) implies the integration of reaction rates, calculated at the reactor intersections. The reaction rates are calculated depending on the type of emission.

5.3.3 Kinetic schemes

An approach was chosen using average reaction rates at the reactor entry and exit planes. By (trapezium rule) integration of these rates across the reactors, a 1-dim kinetics model is obtained.

For a number of species, relations between reaction rate, gas composition and conditions can be derived. With known gas conditions, flow rates at the reactor intersections and reactor lengths, reactor residence times can be calculated and used for integration.

The kinetic scheme reaction rates are functions of temperature and concentrations of species (including radicals) participating in the reaction. Kinetics of radical formation are neglected and equilibrium radical concentrations are assumed. Due to the rapid radical reaction rates relative to residence times in the combustion zones of interest, this is expected to be a good approximation.

Heat release is assumed not to be affected by emission formation itself. Normally, this is a good approximation because exhaust gas emission concentrations are very low.

The generic reactor model algorithm allows easy implementation and adaptation of equations for reaction rates of any specie. For the current multi-reactor model, kinetics calculations are only applied to the emission species NO_x, CO, C_xH_y and Soot (smoke). All other species are assumed to correspond with the chemical equilibrium composition.

Overall emission concentrations result from integration over the reactors.

5.4 NO_x

A NO_x prediction method is used similar to Bozza [5], Fletcher [9] and Barrère [3], and extended with extra chemical reactions and equations.

NO_x concentration is defined as the sum of NO and NO_2. NO_2, if existent, easily reacts to NO at high temperatures. In the flame zone, a portion of NO_2 may remain as a result of sudden chilling (Glassman [10]; Miller [25]). In a combustor dilution zone, NO_2 may also be formed due to a shift of the equilibrium towards NO_2. However, in most cases, the portion of NO_2 is relatively small. Therefore, the sum of NO and NO_2 concentrations is represented by a single NO concentration in the chemical and kinetics models.

N_2O concentration is calculated as an intermediate specie in the NO formation reactions. At the end of the combustor N_2O is only present in very small (calculated equilibrium) concentrations.

All four significant NO_x formation pathways are modeled: prompt, fuel and thermal NO_x and formation via N_2O. Fuel and prompt NO_x formation is assumed instantaneous in the flame zone because both mechanisms are very rapid and involve radicals that are only present in the main fuel reaction zone. This is consistent with the assumption that the combustion process reaches equilibrium instantaneously (see section 5.3).

5.4.1 Prompt NO_x

An equation for prompt NO_x mole concentration is used suggested by Toof [36]:

$$[NO]_{prompt} = X_{CH}\, f(\phi) \sqrt{p}\, [NO]_{eq.stoich} \qquad (3)$$

where:

X_{CH} = mole fraction of hydrocarbon species in fuel,

$f(\phi)$ = a function of ϕ,

p = static pressure (bar).

$[NO]_{eq.stoich}$ = stoïchiometric equilibrium NO concentration.

The empirical equation predicts prompt NO_x formation at combustion of hydrocarbon fuels according to the following reactions:

$$C_2 + N_2 \rightarrow CN + CN \qquad (4)$$

$$C_2H + N_2 \rightarrow HCN + CN \qquad (5)$$

$$CH + N_2 \rightarrow HCN + N \qquad (6)$$

$$CH_2 + N_2 \rightarrow HCN + NH \qquad (7)$$

The radicals formed by reactions (4) through (7) may subsequently oxidize to NO_x.

Prompt NO_x formation via the Zeldovich mechanism with super-equilibrium O and OH radical concentrations and the N_2O mechanism is neglected. This is a good approximation because in flames, super-equilibrium O and OH concentrations are usually only present at temperatures too low for the Zeldovich mechanism (Miller [25]).

The contribution of the N_2O mechanism to prompt NO_x formation is also neglected because it only becomes significant at conditions where total NO_x emissions are very low (Glassman [10]).

An empirical function f(ϕ) (figure 4) is determined using measurement data described in Bachmaier [2] and assumes negligible prompt NO_x formation at equivalence ratios below 0.6 and above 1.65.

However, with gasoline or fuels with significant amounts of ethylene and acetylene in very rich mixtures (i.e. ϕ>1.65), significant prompt NO_x may well be formed and then equation (3) will underestimate prompt NO_x.

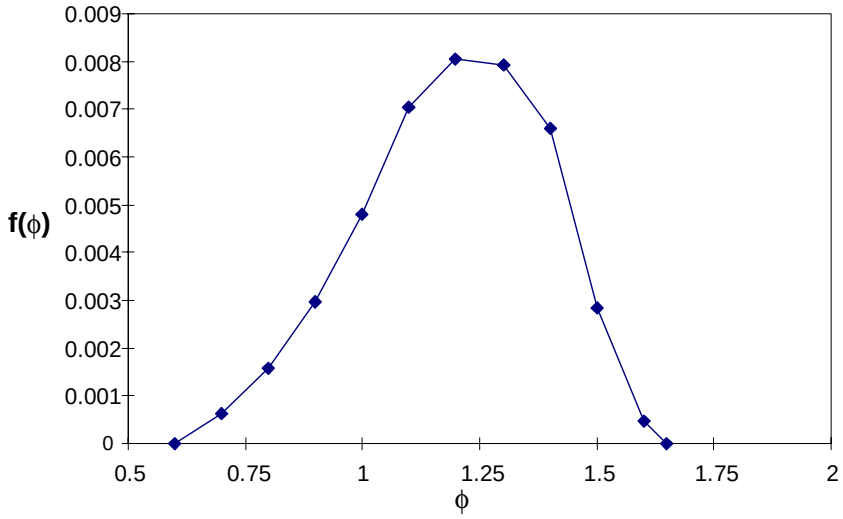

Figure 4 Prompt NO_x factor function

5.4.2 Fuel NO_x

Fuel NO_x formation is specified with the *conversion fraction*, i.e. the fraction of total fuel bound nitrogen that is actually converted to NO_x. Glassman [10] and Fenimore [8] indicate that the conversion fraction seems independent of the way nitrogen is chemically bound in the fuel, but it strongly depends on the combustion environment (e.g. equivalence ratio and fuel composition). Experiments by Kelsall [18], Sato [32], Nakata [27] and Fenimore [8] indicate large differences in conversion fractions depending on many different factors. It was therefore decided to apply a user specified conversion fraction for the model at this stage. The fraction of fuel-bound nitrogen in the fuel is also user-specified.

5.4.3 Thermal NO_x

For both the thermal and N_2O mechanisms, a reaction scheme is used to derive an equation for NO formation rate, required for integration across the subsequent reactors. Thermal NO_x formation rate is predicted according to the extended Zeldovich mechanism:

$$N_2 + O \leftrightarrow NO + N \quad (8)$$

$$N + O_2 \leftrightarrow NO + O \quad (9)$$

$$N + OH \leftrightarrow NO + H \quad (10)$$

5.4.4 N_2O mechanism

For the N_2O mechanism's contribution to the NO_x formation rate the following reactions are included:

$$N_2O + M \leftrightarrow N_2 + O + M \quad (11)$$

$$N_2O + O \leftrightarrow N_2 + O_2 \quad (12)$$

$$N_2O + O \leftrightarrow NO + NO \quad (13)$$

$$N_2O + H \leftrightarrow N_2 + OH \quad (14)$$

$$N_2O + H \leftrightarrow NO + NH \quad (15)$$

$$N_2O + CO \leftrightarrow NO + NCO \quad (16)$$

The NO_x formation rate equation is derived according to Barrère [3] although more reactions are included. All the species are assumed to be in equilibrium, except for NO, N_2O and N.

"One-way equilibrium reaction rates" (Fletcher [9]) represent the forward and backward reaction rates of reactions 8 through 16 when equilibrium is assumed. For reaction r, with on the left of the reaction equation, n species with concentrations $[X_1]$ to $[X_n]$, the (one way) equilibrium reaction rate is:

$$R_r = k_f \prod_{i=1}^{i=n} [X_i]_{eq} \quad (17)$$

k_f is the *forward* specific reaction rate constant (Arrhenius law):

$$k = AT^B e^{-\frac{E_a}{RT}} \quad (18)$$

A, B are constants, E_a is the activation energy and R is the gas constant. The equilibrium reaction rate R_r can also be calculated using the concentrations on the *right* of the equation and the *backward* specific reaction rate constant.

The factors α, β and γ represent the deviation from equilibrium of the *actual* NO, N and N_2O concentrations at a time t during integration:

$$\alpha = \frac{[NO]}{[NO]_{eq}} \tag{19}$$

$$\beta = \frac{[N]}{[N]_{eq}} \tag{20}$$

$$\gamma = \frac{[N_2O]}{[N_2O]_{eq}} \tag{21}$$

From the above equations then the following equations for the reaction rates can be derived:

$$\frac{d[NO]}{dt} = R_8 + \beta(R_9 + R_{10}) + \gamma(2R_{13} + R_{15} + R_{16}) - \alpha(\beta R_8 + R_9 + R_{10} + 2\alpha R_{13} + R_{15} + R_{16}) \tag{22}$$

$$\frac{d[N]}{dt} = R_8 + \alpha(R_9 + R_{10}) - \beta(\alpha R_8 + R_9 + R_{10}) \tag{23}$$

$$\frac{d[N_2O]}{dt} = R_{11} + R_{12} + R_{14} + \alpha(\alpha R_{13} + R_{15} + R_{16}) - \gamma(R_{11} + R_{12} + R_{13} + R_{14} + R_{15} + R_{16}) \tag{24}$$

The N and N_2O concentrations may well assumed to be in steady state (Lavoie [21] and Botros [4]). With this assumption, the left-hand sides of equations (23) and (24) are zero, and β and γ are found as a function of α and the relevant one-way equilibrium reaction rates. After substitution of β and γ in equation (22), the following equation is found for the NO formation rate:

$$\frac{d[NO]}{dt} = 2(1-\alpha^2) * \left\{ \frac{R_8}{1 + \alpha \dfrac{R_8}{R_9 + R_{10}}} + \frac{R_{13} + \dfrac{R_{15} + R_{16}}{2(1+\alpha)} \left(1 + \dfrac{\alpha R_{13}}{R_{11} + R_{12} + R_{14}} \right)}{1 + \dfrac{R_{13} + R_{15} + R_{16}}{R_{11} + R_{12} + R_{14}}} \right\} \tag{25}$$

Equation (25) can directly be used in the integration in the reactor model. The one-way equilibrium reaction rates can directly be calculated from gas conditions and equilibrium composition, and α results from the actual NO concentration as calculated in the previous integration step.
The first term between the curly brackets represents thermal NO_x formation, while the second term relates to the N_2O mechanism.
Because the one-way equilibrium reaction rates can be calculated using either the forward or backward reaction, the number of equilibrium concentrations to be calculated can be limited to only the NO and N_2O equilibrium concentrations.

5.5 CO

For the carbon monoxide emission calculation, the assumption is made that during combustion, fuel first reacts to all CO and water. After this initial and instantaneous step, CO further reacts to CO_2 depending on reaction rates calculated in the reactor models. This approach is based on the fact that oxidation to CO is very rapid relative to oxidation from CO to CO_2, (Sturgess [35], Hammond [12] and Westenberg [38]). The reaction scheme is used for CO emission calculation only and does not affect heat release. Also the CO formation rate still depends on equilibrium temperature level.
The reaction to CO_2 is assumed to take place according to the dominant mechanism at CO oxidation (Westenberg [38]; Dryer [7]):

$$CO + OH \longleftrightarrow CO_2 + H \tag{26}$$

Chleboun [6] proposes the following equation for the rate of carbon monoxide oxidation assuming H and OH equilibrium concentrations and a separate conservation of carbon atoms for this mechanism:

$$\frac{d[CO]}{dt} = -k_{26f}[OH]_{eq} * \left\{1 + \frac{[CO]_{eq}}{[CO_2]_{eq}}\right\}\left([CO] - [CO]_{eq}\right) \tag{27}$$

In this equation, the k_{26f} is the specific forward reaction rate constant of equation (26). The equation is integrated across the combustion chamber reactors similar to the method for NO_x.
Equation (27) is able to model the effect of rapid reaction down towards equilibrium CO concentrations at relatively high temperatures and also to simulate the effect of frozen high CO concentrations due to sudden quenching. In the latter case, the reaction rate constant will suddenly decrease to a very low value, thereby preventing further rapid CO oxidation.

5.6 UHC

To predict the emission levels of unburned hydrocarbons, reaction rates are integrated starting at an initial concentration corresponding with the fuel flow entering the reactor. Two different reactions are used. Jet-A fuel may well be represented by $C_{12}H_{23}$ (NASA publications: Gordon [11]; McBride [24]) which initially reacts according to:

$$C_{12}H_{23} + 6O_2 \rightarrow 12CO + 11.5H_2 \tag{28}$$

Other jet and diesel fuels are assumed to react according to this reaction also. In Pratt [29], the following equation is proposed for the rate of this reaction:

$$\frac{d[C_{12}H_{23}]}{dt} = -10^{11.5}\left(\frac{p}{p_0}\right)^{-0.815} * e^{\left(-\frac{12200}{T}\right)}\left[\frac{9T}{10^4} - \frac{1}{2}\right]\sqrt{[C_{12}H_{23}]}[O_2] \tag{29}$$

For natural gas and other hydrocarbon gas fuels, the flow of hydrocarbons entering the combustion chamber is converted to a concentration of methane assuming that the molar mass of the hydrocarbons is the same as the methane molar mass. The burning rate of methane is taken from Dryer [7]:

$$\frac{d[CH_4]}{dt} = -10^{10.2} e^{\left(-\frac{48400}{RT}\right)}[CH_4]^{0.7}[O_2]^{0.8} \tag{30}$$

The UHC level is found by integrating either equation (29) or (30) depending on the fuel type.

5.7 Smoke

The smoke emission model is based on a number of properties described by Appleton [1]. It appears that the soot formed in flames only weakly depends on the conditions where it is formed. For example, the soot formation is hardly affected by the type of flame (premixed or diffusion). Soot primarily contains carbon, although also hydrogen and oxygen can be present. Concerning structure, soot particles are roughly spherical and grouped together in a “necklace-like” fashion. The smoke model again utilizes the assumption of instantaneous formation followed by subsequent oxidation according to the kinetics mechanism in the generic reactors. The formation model is derived from an empirical equation taken from Rizk [30] predicting both formation and oxidation. The equation’s term for oxidation is omitted resulting in the following equation:

$$S = 0.0145 \cdot \frac{\phi \cdot FAR_{stoich} p_3^2}{W_{ox} T} (18 - H)^{1.5} \quad (31)$$

p_3 = burner pressure (kPa), W_{ox} = oxidant mass flow (kg/s), T reaction end temperature (K), H = fuel hydrogen mass percentage. The term for fuel air ratio has been replaced by the equivalence ratio multiplied with the stoïchiometric fuel air ratio. This results in a more generic representation of the fuel air ratio relative to a stoïchiometric mixture and allows for oxidants and fuels other than pure air and jet fuel.

Equation (31) is based on measurements in diffusion flame combustion chambers and because the soot formation process is relatively poorly understood, it can only be roughly predicted with this equation.

The soot oxidation process is much better understood and can be modeled using equations for the overall specific surface reaction rate developed by Nagle and Strickland-Constable [26]:

$$\omega = 12x\left[\frac{k_A p_{O_2}}{1 + k_Z p_{O_2}}\right] + k_B p_{O_2}(1 - x) \quad (32)$$

with:

$$x = \frac{1}{1 + \frac{k_T}{p_{O_2} k_B}} \quad (33)$$

$$k_A = 20\, e^{\left(-\frac{30}{RT}\right)} \quad (34)$$

$$k_B = 4.46 \cdot 10^{-3}\, e^{\left(-\frac{15.2}{RT}\right)} \quad (35)$$

$$k_T = 1.51 \cdot 10^5\, e^{\left(-\frac{97}{RT}\right)} \quad (36)$$

$$k_Z = 213\, e^{\left(\frac{4.1}{RT}\right)} \quad (37)$$

ω is Specific surface oxidation rate (g/cm^2/s), p_{O2} is partial pressure (atmospheres) of O_2. For validation and explanation of these semi-empirical equations refer to Appleton [1].

The smoke calculation procedure is as follows. First, the smoke (mass) formation calculated with equation (31) is converted into a number of spherical smoke particles per unit of combustion gas. This number depends on a user specified initial radius of the spheres, which

usually should be around 40 nm. The smoke particles are then oxidized in the subsequent reactors. The smoke surface oxidation rate is calculated using equation (32). Applying a constant average soot density of 1800 (kg/m^3), this surface oxidation rate is converted into a rate of radius change. At the end of the combustion chamber the number of spherical particles and their radii are used to find the “particulate mass loading” (for the smoke number). In the case where new particles are emitted in subsequent combustion stages (e.g. in multi-stage combustors), particles with different radii would exist. In that case, a weighted averaged radius is used to continue calculation.

6 Considerations for building a model

For application of GSP's new combustor model to predict emissions the following issues need to be considered:

- In general, it is best to use the model corresponding to GSP's general way of use: i.e. as a sensitivity analysis tool instead of a direct prediction tool. Accurate analysis can be made of effects of a large variety of operating conditions on emission levels.
- For off-design analysis, reference emission data are required as well as combustor data.
- The emission model can be tuned to the reference data using unknowns like geometric reactor data (determining residence times), flow distribution factors and a number of other parameters depending on the emission type.
- At this stage, flow distribution is specified with constant factors. Until a combustor operating condition dependent flow distribution model is available, the implications of this limitation must be considered for large deviations from the reference combustor flow conditions.
- CO, UHC and Smoke emissions are to a large extent caused by effects that cannot be easily simulated with one-dimensional models (e.g. combustor liner cooling, atomization etc.). Therefore "temperature tuning factors" have been added to represent deviations from equilibrium temperatures at the reactor intersections. These factors will typically be used to represent effects like cooling flow films on average temperatures. Temperature factors may be set for all emission types at every reactor intersection and can also be used for NO_x. A temperature factor of 1 indicates unmodified equilibrium temperature is used.
- Specific attention must be paid to the multi-reactor configuration. With only two reactors, the combustor processes can only be simulated to a very limited extent. With a large number of reactors, several effects like varying dilution ratios, residence times, temperatures etc. can be calculated accurately.
- Direct prediction of emissions is possible if limited (geometric) combustor data are available but will only provide reasonable estimates for NO_x emission levels.
- Accurate simulation of combustor operating conditions is required for deriving the correct relation between engine operating conditions and emissions. This requires a validated GSP thermodynamic model.
- The model may be particularly valuable for coupling detailed CFD calculation results to general gas turbine performance models. In this case combustor CFD results must be transformed into an accurately tuned GSP multi-reactor model.

7 Results

Extensive validation of the models will be the subject of future work, requiring the acquirement and analysis of detailed gas turbine data. However, the new model has been applied to a number of gas turbine engines to demonstrate the analysis of a variety of problems.

7.1 Deterioration in a large turbofan engine

First, the ability of the model to predict emissions of a large turbofan engine (GE CF6-80C2) was tested. Emission data from the ICAO databank [15] and (especially low power setting) test bed measurement data were used for validation. The combustor was modelled with three reactors (figure 5). The data required at the intersections are given in table 1.

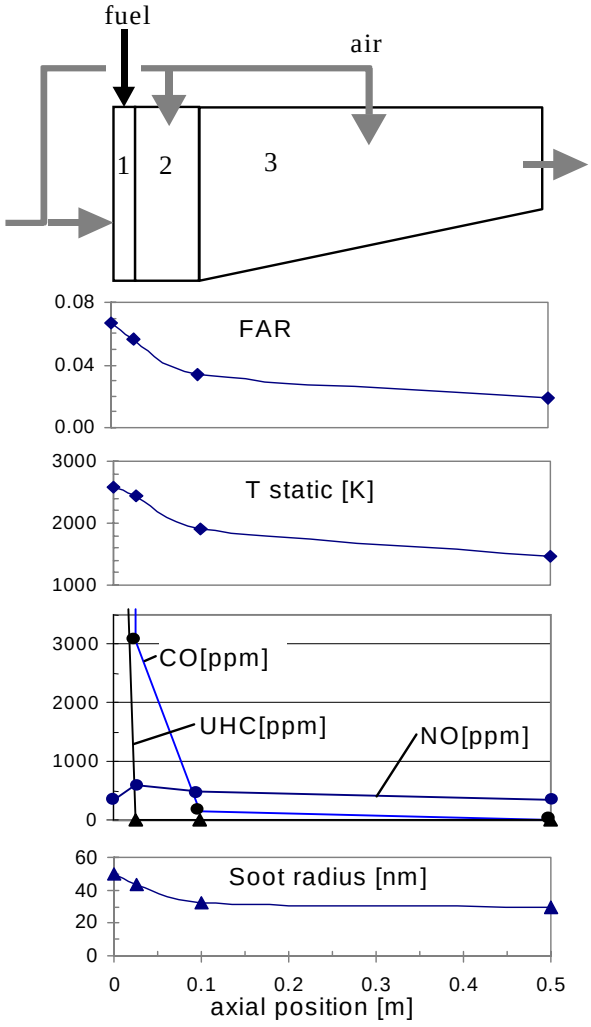

Figure 5 CF6-80C2 3-reactor combustor model and design point results

Initial soot radius was set to 50 nm. Little was known about the flow distribution within the combustor and therefore stoïchiometric primary zone (first reactor) fuel-air ratio was assumed for the design point (sea level static rated thrust) at this stage. Limited tuning with temperature factors (see section 6) was applied for the NO_x and UHC emissions.

Table 1 CF6-80C2 combustor model data

Zone	Flow area (m^2)	reactor length (m)	Air inflow fraction
Flame front	0.360		0.28
Primary	0.360	0.025	0.05
Secondary	0.360	0.074	0.22
Dilution	0.1653	0.4	0.45

Figure 5 shows fuel-air ratio (FAR), temperature, emission concentrations and soot radius as calculated at the 4 intersections along the axial in the design (reference) operating point.

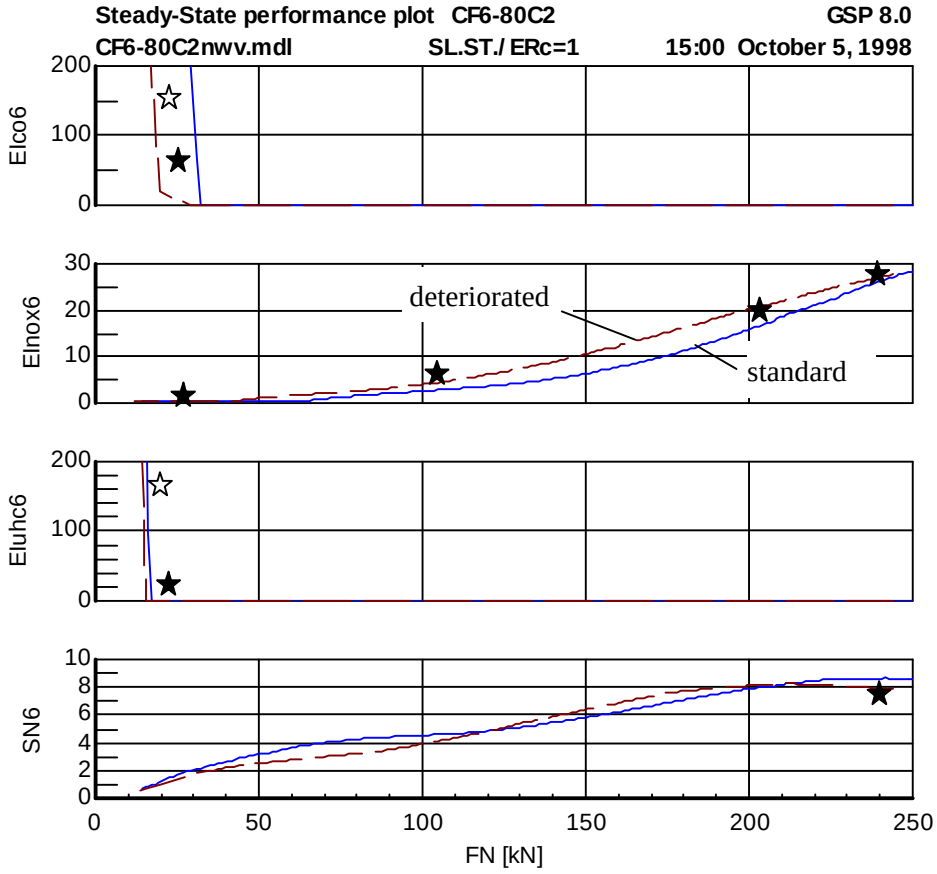

Figure 6 CF6-80C2 emission results and deterioration effects

In figure 6 emissions calculation results are presented for standard conditions (solid curves) and for the case of a deteriorated high-pressure turbine (dashed line) to demonstrate typical use of the model. Turbine deterioration is represented by a 4% lower isentropic efficiency combined with a 2% increase in flow. The solid lines should correspond with data from the ICAO databank (★) and with test-bed measured data (☆, for the low power settings). The NO_x prediction matches the data along the operating range. UHC emissions only become significant in a narrow low power range, which is well predicted by the model. Significant CO emissions are predicted to occur at slightly higher power settings than those of the reference data. The single smoke number (SN6) value that was available could accurately be matched.
The effects of turbine deterioration are as expected: due to higher combustor temperature levels, higher NO_x and lower CO and UHC emissions. Note that at high power setting, the NO_x increase becomes smaller due to the richer primary zone with a deteriorated turbine. Other results with rich (instead of stoïchiometric) primary zone mixtures (in the design point) even indicated a fall in NO_x with turbine deterioration, resulting from the then dominant effect of decreasing combustion temperatures with equivalence ratios increasing beyond 1. Smoke number values could only be validated against the take-off power value (i.e. 7.1) from the ICAO databank [15].

7.2 Alternative fuel for an industrial gas turbine engine

A second application is the analysis of the effect of low calorific fuel (LCV, 15.6% CO_2, 8.8% CO, 24% steam, 7.4% H_2, 5.2% CH_4, 0.3% C_2H_6, 1.1% C_2H_4, 37.6% N_2) obtained from a bio-mass gasifier at Delft University of Technology (Hoppesteyn [14]; de Jong [17]), if used for a GE-LM2500 class LNG-fuel industrial turboshaft engine.
The gasified fuel heating value is only about 1/10 of the LNG heating value, delivery pressure is 5 bar and temperature is 1073 K. Separate compressors are assumed to compress the gasifier air and fuel gas for injection into the combustor. With the large amount of (hot) fuel gas this requires a considerable quantity of power to be taken from the power turbine drive shaft, leaving Pnetc as net power output[2].The effect on both thermodynamic performance and emissions was calculated (LCV=dashed curves) and compared to normal operation with LNG (solid curves). In figure 7 the effect on performance is presented with net power output Pnetc on the X-axis. The third graph shows the high LCV fuel compression power Pcfuel. The TT4.5 power turbine entry temperature curves indicate similar turbine temperature levels for both fuels.

[2] This case may not represent an optimal configuration but only serves to demonstrate the potential of the model.

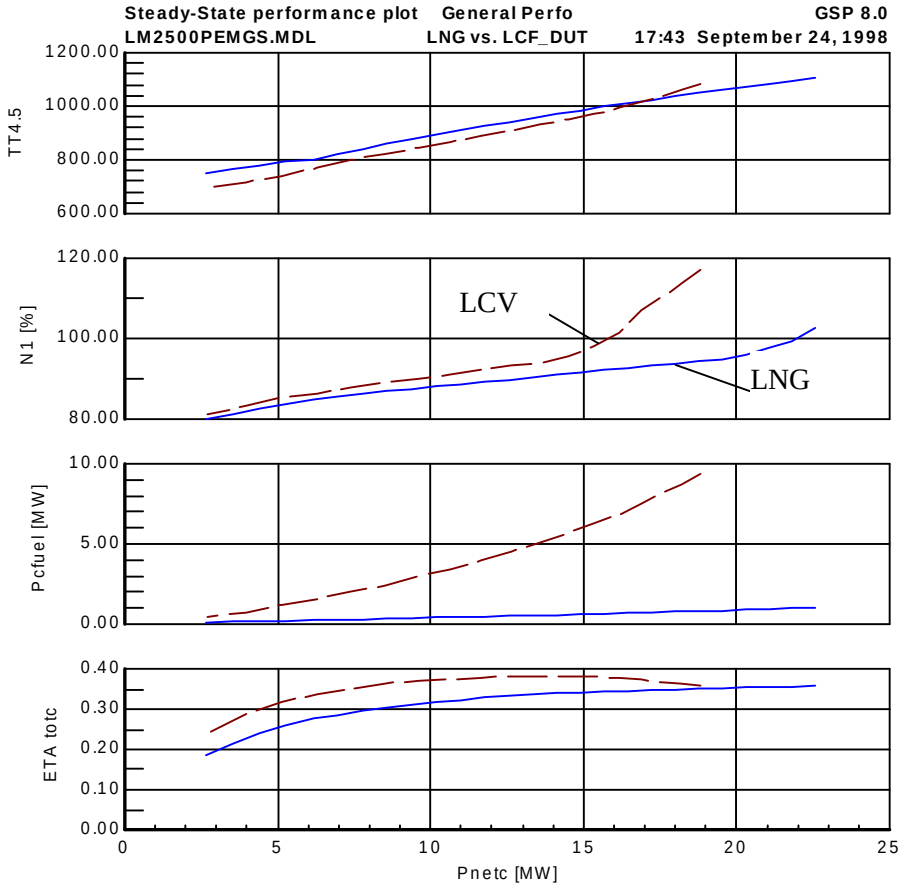

Figure 7 Effects on general performance of LCV

An important outcome is that nominal power cannot be obtained without exceeding the compressor speed (N1) limit. This is due to the mismatch between compressor and HP turbine power resulting from the large fuel mass flow injected into the combustor. Unless compressor load is increased (e.g. by taking compressor bleed air to feed to the gasifier) or major hardware modifications are applied (turbine flow capacity), lower net power output must be accepted. It should be noted that with a fixed power turbine (i.e. a single shaft engine) this problem will not occur; but then stall-margin problems are likely to emerge instead. Total efficiency (ETAtotc, corrected for required fuel compression power) shows favorable values at partial power levels, but this may well have to be corrected with extra power required for the gasifier.

A major concern will be how the compressor operating line will be affected. Figure 8 shows the expected shift towards the surge line, possibly resulting in implications with regard to (turbine) hardware modifications.

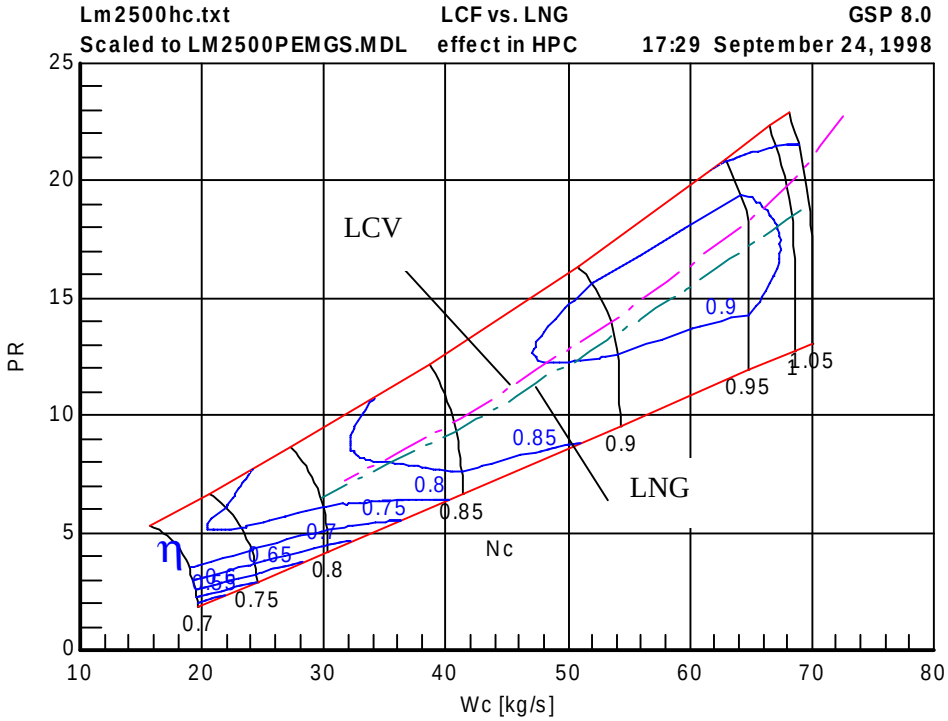

Figure 8 LCV vs. LNG fuel HPC operating lines

Finally, the effects on emission levels are predicted using the multi-reactor emission model with similar characteristics as those of the above-mentioned CF6-80C2 model, assuming a similar global combustor geometry.

The top graph in figure 9 shows the large LCV fuel mass flow Wf4 (to be multiplied with the EI indices for total emission output by mass). The next graph shows the much lower primary zone temperature T_{pz}, causing virtually no (thermal) NO_x emission with LCV at equal power levels (as compared to LNG fuel, 3rd graph in figure 9).

The lower T_{pz} values with LCV fuel are due to the large portions of N_2, CO_2 and H_2O in the LCV fuel "cooling" the combustion process, resulting in a low adiabatic flame temperature. Finally, the high CO emission at low power (4th graph in figure 9), only with LCV, is due to the low CO reaction rate at lower temperatures.

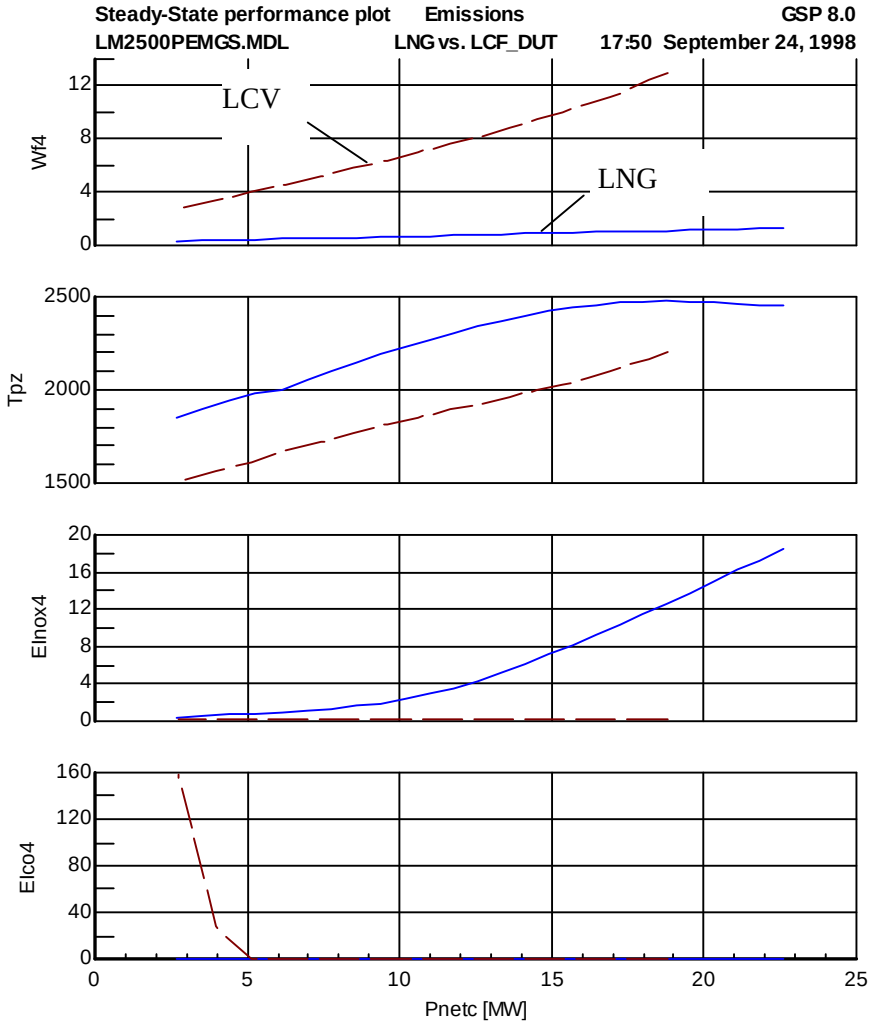

Figure 8 LCV vs. LNG fuel exhaust gas emissions

8 Conclusions

The GSP gas turbine simulation environment, after being extended with a detailed composition specific gas model, is a powerful tool to predict effects of alternative fuels on performance and emissions.

The new multi-reactor combustor model is a generic structure in which 1-dim kinetic models can be implemented for formation of various species including the major exhaust gas emissions. For NO_x, CO, UHC and Smoke, models have been developed for instantaneous formation in the flame zone and subsequent formation or reaction according to multi-reactor kinetics schemes

It should be noted that in general these models are best used as sensitivity analysis tools, i.e. to calculate effects on performance and emission parameters relative to reference values.

A useful application of the new gas model has been demonstrated in the analysis of the effect of low calorific gas from a bio-mass gasifier on various performance parameters and emissions. This type of performance analysis may well be used to support decisions concerning engine hardware modifications.

The emission models have also been demonstrated on a large turbofan engine. The results corresponded with measured emission data and with expected operating condition effects on emissions. With the NO_x model best accuracy was obtained. The accuracy of particularly the CO, UHC and Smoke formation models may be improved by adapting the multi-reactor model to allow for modelling of effects such as film cooling and other effects not covered by a one-dimensional model. In particular, a flow distribution model depending on a variety of conditions in the combustor must be developed to allow for large deviations from the reference conditions.

More work needs to be done to validate results using detailed combustor data of a variety of engines and operating conditions. The generic set-up of the model allows easy implementation of improved emission models.

Interesting future applications include performance analysis of LH_2 and LNG fueled aero-engines and a variety of alternative fuel solutions for land based gas turbines.

9 References

1) Appleton, J.P., 'Soot oxidation kinetics at combustion temperatures', *Atmospheric Pollution by Aircraft Engines, AGARD-Conference Proceedings-125*, paper 20. Neuilly Sur Seine: AGARD, 1973.
2) Bachmaier, F., Eberius, K.H., Just, Th., 'The formation of Nitric Oxide and the detection of HCN', *Combustion Science and Technology*, vol.7, p.77. New York: Gordon and Breach Science Publishers Ltd., 1973.
3) Barrère, M., 'Modélisation des foyers de turboréacteur en vue de l'étude de la pollution', *Atmospheric Pollution by Aircraft Engines, AGARD-Conference Proceedings-125*, paper 27. Neuilly Sur Seine: AGARD, 1973. (in French)
4) Botros, M.J., et al., 'One-dimensional predictive emission monitoring model for gas turbine combustors', ASME Paper 97-GT-414, *ASME Technical Papers*, New York: ASME, 1997.
5) Bozza, F., Tuccillo, R., Fontana, G., 'Performance and Emission Levels in Gas Turbine Plants', *Journal of Engineering for Gas Turbines and Power*, vol.116, p.53-62. New York: ASME, 1994.
6) Chleboun, P.V., Hubbert, K.P., Sheppard, C.G.W., 'Modelling of CO Oxidation in Dilution Jet Flows', *Combustion and Fuels in Gas Turbine Engines, AGARD-Conference Proceedings-422*, paper 38. Neuilly Sur Seine: AGARD, 1988.
7) Dryer, F.L., Glassman, I., 'High-Temperature oxidation of CO and CH_4', *Pollutant Formation and Destruction in flames, 14th Symposium (Int.) on Combustion*, p.987-1003. Pittsburgh: The Combustion Institute, 1973.
8) Fenimore, C.P., 'Formation of Nitric Oxide from Fuel Nitrogen in Ethylene Flames', *Combustion and Flame*, vol.19, p.289-297. New York: American Elsevier Publishing Company Inc., 1972.
9) Fletcher, R.S., Heywood, J.B., 'A model for nitric oxide emissions from aircraft gas turbine engines', AIAA Paper 71-123, *AIAA Technical Papers*. New York: AIAA, 1971.
10) Glassman, I., *Combustion.* Princeton NJ, USA: Academic Press, 1996.
11) Gordon, S., McBride, B.J., *Computer Program for Calculation of Complex Chemical Equilibrium Compositions and Applications. I. Analysis.* NASA Reference Publication 1311. Ohio, National Aeronautics and Space Administration, Lewis Research Center, 1994.
12) Hammond, D.C. JR., Mellor, A.M., 'Analytical Calculations for the Performance and Pollutant Emissions of Gas Turbine Combustors', *Combustion Science and Technology*, vol.4, p.101-112. New York: Gordon and Breach Science Publishers Ltd., 1971.
13) Holderness, F.H., Macfarlane, J.J., 'Soot Formation in Rich Kerosine Flames at High Pressure', *Atmospheric Pollution by Aircraft Engines, AGARD Conference Proceedings-125*, paper 18. Neuilly Sur Seine: AGARD, 1973.

14) Hoppesteyn, P.D.J., Andries, J., Hein, K.R.G., 'Biomass/coal derived gas utilization in a gas turbine combustor', ASME Paper 98-GT-160, *ASME Technical Papers*. New York: ASME, 1998.

15) 'ICAO Engine Exhaust Emissions Data Bank', issue 1, 1993, Appendix C, data for CF6-80C2B1F, page C-41.

16) Jentink, H.W., Veen, J.J.F. van, 'In flight spectroscopic aircraft emission measurements'. To be published in the proceedings of this symposium *Gas Turbine Engine Combustion, Emissions and Alternative fuels*. Neuilly Sur Seine: RTO, 1998.

17) Jong, W. de, Andries J., Hein, K.R.G., 'Coal-biomass gasification in a pressurized fluidized bed gasifier', ASME Paper 98-GT-159, *ASME Technical Papers*. New York: ASME, 1998.

18) Kelsall, G.J., et al., 'Combustion of LCV Coal Derived Fuel Gas for High Temperature, Low Emissions Gas Turbines in the British Coal Topping Cycle', ASME Paper 91-GT-384, *ASME Technical Papers*. New York: ASME, 1991.

19) Kretschmer, D., Odgers, J., 'The characterization of combustion by fuel composition – measurements in a small conventional combustor', *Combustion and Fuels in Gas Turbine Engines, AGARD-Conference Proceedings-422*, paper 10. Neuilly Sur Seine: AGARD, 1988.

20) Kuo, K.K., *Principles of Combustion*. New York: John Wiley & Sons, 1986.

21) Lavoie, G.A., Heywood, J.B., Keck, J.C., 'Experimental and Theoretical Study of Nitric Oxide formation in Internal Combustion Engines', *Combustion Science and Technology*, vol.1, p.313-326. New York: Gordon and Breach Science Publishers Ltd., 1970.

22) Lefebvre, A.W., *Gas Turbine Combustion*. Washington: Hemisphere Publishing Corporation, 1983.

23) Maidhof, S., Janicka, J., 'Numerical modelling of turbine combustion chambers', *Fuels and Combustion Technology for Advanced Aircraft Engines, AGARD-Conference Proceedings-536*, paper 10. Neuilly Sur Seine: AGARD, 1993.

24) McBride, B.J., Gordon, S., Computer Program for Calculation of Complex Chemical Equilibrium Compositions and Applications. II. Users Manual and Program Description. NASA Reference Publication 1311. Ohio, National Aeronautics and Space Administration, Lewis Research Center, 1996.

25) Miller, J.A., Bowman, C.T., 'Mechanism and modelling of nitrogen chemistry in combustion', *Progress in Energy and Combustion Science*, vol.15, p.287-338. Oxford: Pergamon Press plc., 1989.

26) Nagle, J., Strickland-Constable, R.F., 'Oxidation of carbon between 1000°C-2000°C', *Proceedings 5th Conference on Carbon*, page 154, Pergamon, 1961.

27) Nakata, T., et al., 'Experimental Evaluation of a Low NO_x LBG Combustor Using Bypass Air', ASME Paper 90-GT-380, *ASME Technical Papers*. New York: ASME, 1990.

28) Pohl, H.W., (editor) Hydrogen and Other Alternative fuels for Air and Ground Transportation. Chichester, UK: John Wiley & Sons Ltd., 1995.

29) Pratt, D.T., 'Coalescence/Dispersion Modelling of Gas Turbine Combustors', *Combustor Modelling, AGARD-Conference Proceedings-275*, paper 15. Neuilly Sur Seine: AGARD, 1980.

30) Rizk, N.K., Mongia, H.C., 'Emissions Predictions of Different Gas Turbine Combustors', AIAA Paper 94-118, *AIAA Technical Papers*. New York: AIAA, 1994.

31) Rodriguez, C.G., O'Brien, W.F., 'Unsteady, finite-rate model for application in the design of complete gas-turbine combustor configurations', *Design principles and methods for aircraft gas turbine engines, AGARD Conference Proceedings*. Neuilly Sur Seine: RTO, 1998.

32) Sato, M., et al., 'Coal Gaseous Fueled, Low Fuel-NO_x Gas Turbine Combustor', ASME Paper 90-GT-381, *ASME Technical Papers*. New York: ASME, 1990.

33) Schumann, U., (editor) Lecture Notes in Engineering. Air Traffic and the Environment-Background, Tendencies and Potential Global Atmospheric Effects. Berlin: Springer-Verlag, 1990.

34) Schumann, U., AERONOX, The impact of NOx Emissions from Aircraft Upon the Atmosphere at Flight Altitudes 8-15 km, EC-DLR Publication on research related to aeronautics and environment. DLR, Germany, 1995.

35) Sturgess, G.J., McKinney, R., Morford, S., 'Modification of Combustor Stoïchiometry Distribution for Reduced NOx Emission From Aircraft Engines', ASME Paper 92-GT-108, *ASME Technical Papers*, New York: ASME, 1992.

36) Toof, J.L., 'A Model for the Prediction of Thermal, Prompt, and Fuel NO_x Emissions From Combustion Turbines', ASME Paper 85-GT-29, *ASME Technical Papers*. New York: ASME, 1985.

37) Visser, W.P.J., 'Gas Turbine Simulation at NLR', 'Making it REAL', *CEAS Symposium on Simulation Technology* (paper MOD05), Delft, the Netherlands, 1995.

38) Westenberg, A.A., 'Kinetics of NO and CO in Lean, Premixed Hydrocarbon-Air Flames', *Combustion Science and Technology*, vol.4, p.59-64. New York: Gordon and Breach Science Publishers Ltd., 1971.